Theor Chem Acc (2004) 112: 335–341
DOI 10.1007/s00214-004-0593-0

Theoretical
Chemistry Accounts

Regular article

Complete-active-space self-consistent-field/Amber parameterization of the Lys296–retinal–Glu113 rhodopsin chromophore-counterion system

Nicolas Ferré[1], **Alessandro Cembran**[2], **Marco Garavelli**[2], **Massimo Olivucci**[1,3]

[1] Dipartimento di Chimica, Università di Siena, via Aldo Moro, 53100 Siena, Italy
[2] Dipartimento di Chimica "G. Ciamician", Università di Bologna, via Selmi 2, 40126 Bologna, Italy
[3] Centro per lo Studio dei Sistemi Complessi, via Tommaso Pendola 37, 53100 Siena, Italy

Received: 17 July 2003 / Revised version: 18 December 2003 / Published online: 30 July 2004

Abstract. A special hybrid quantum mechanics/molecular mechanics forcefield is defined, parameterized and validated for studying the photoisomerization path of the retinal chromophore in the rhodopsin protein. It couples a multireference ab initio Hamiltonian (CASSCF and second-order multireference many-body perturbation theory using a CASSCF reference) to describe the chromophore while the rest of the protein is approximated with the Amber forcefield. The frontier has been carefully parameterized in order to reproduce full quantum mechanics torsional energy profiles, for both the ground state and the first excited state. It is also shown that replacing the chromophore counterion with point charges is a valid approximation. This result is interpreted in terms of a cancellation effect for which a possible explanation is given.

Keywords: Rhodopsin – Retinal – Photoisomerization – Quantum mechanics/Molecular mechanics – Parameterization

1 Introduction

The primary event in the vision process consists in the ultrafast photoisomerization of the retinal chromophore of the protein rhodopsin [1,2], a member of the G-protein coupled receptor family. In the so-called dark state of rhodopsin, the chromophore is in its 11-cis form. After absorption of a photon (the maximum absorption wavelength is about 500 nm), this isomerizes to its all-trans form, producing the low temperature stable intermediate "bathorhodopsin" in picoseconds. On the other hand, it is now established that the formation of bathorhodopsin is preceded by the ultrafast (200 fs) production of a transient precursor called "photorhodopsin". The elusive geometrical and electronic structure of this "primary" transient species has not yet been elucidated and this is where computational (photo)chemistry can give considerable insights.

Computational studies have mainly focused on the retinal chromophore in vacuo and the corresponding photoisomerization mechanism is now established. Indeed, static and dynamical studies have been performed that validate a two-states two-modes mechanism [3, 4, 5, 6, 7]. However, the influence of the protein on the mechanism of this reactive process is still largely unknown. Only few theoretical papers have been published on this topic [8, 9, 10, 11, 12], mainly owing to the lack of a reasonable threedimensional structure of rhodopsin. On the other hand, the recently published 2.8Å resolved structure [13, 14] provides the first step towards the definition of a realistic computational model of the protein.

The present paper presents a detailed report of part of the initial work we have carried out to derive a suitable hybrid quantum mechanics (QM)/molecular mechanics (MM) model of rhodopsin that has recently been used in a successful investigation of its spectroscopy [15]. This model is based on a complete-active-space-self-consistent-field (CASSCF) QM part and a MM part based on the Amber forcefield. The CASSCF was chosen because one is interested in describing the relaxation of the excited state via a second-order multireference many–body perturbation theory using a CASSCF reference (CASPT2//CASSCF) computational strategy. Even if the new parameters have already been given and used [15], the present work emphasizes the procedure followed to derive this hybrid QM/MM forcefield and the validation tests performed to check its accuracy. In particular, we focus on the Lys296–retinal–Glu113 chromophore-counterion system of the protein.

2 The model

The retinal chromophore is covalently linked to a lysine residue (Lys296) of the protein through the protonated Schiff base function, whose counterion is a glutamate residue (Glu113). Besides the nonbonded interactions

Correspondence to: M. Olivucci
e-mail: olivucci@unisi.it

between the chromophore and the residues of the protein pocket and the long-range electrostatic interactions of the chromophore with the entire protein–solvent–membrane macromolecular system, this lysine–retinal–glutamate (LRG) system may be considered the source of the zeroth order interaction between the isolated chromophore and the protein cavity. As such it is held responsible for a large part of the force that drives the initial photoisomerization motion. Thus, in order to derive a reliable QM/MM model of rhodopsin one has first to focus on this LRG molecular group (i.e. one must propose a model which combines the accuracy of the calculated properties and the computational tractability). While the protein bulk will be treated using a standard MM forcefield, we present a LRG QM/MM potential in which particular attention has been paid to (1) the definition of the size of the QM subsystem with respect to the QM method and computational cost, (2) the design of the QM/MM frontier, (3) the choice of the MM forcefield and (4) the reparameterization of some QM/MM potentials. Concerning the last point, we modified a number of MM classical parameters, in order to reproduce qualitatively the pure QM forcefield of the LRG group. *This means that the QM/MM force field that we want to design will be accurate but strongly problem dependent*. It would be difficult to have a less-specific force field, because we are interested in the description of a specific chemical process – the photoisomerization of the retinal chromophore – that involves at least two energy surfaces, while standard forcefields, including the usual MM ones, deal with only one surface (usually the ground-state surface). Furthermore, MM forcefields only deal with conformational (not reactive) changes.

2.1 The QM/MM Hamiltonian

The QM/MM force field is characterized by a special Hamiltonian which is the sum of three terms:

$$\hat{\mathbf{H}} = \hat{\mathbf{H}}_{QM} + \hat{\mathbf{H}}_{MM} + \hat{\mathbf{H}}_{QM/MM} \tag{1}$$

On the right-hand side, $\hat{\mathbf{H}}_{QM}$ is the usual Hamiltonian of the QM part as if it were in vacuo, $\hat{\mathbf{H}}_{MM}$ is actually the classical energy of the MM part and $\hat{\mathbf{H}}_{QM/MM}$ takes into account all the interactions between the QM and MM subsystems. Given n electrons and N nuclei interacting with Q point charges, this last term can be split into several contributions:

$$\hat{\mathbf{H}}_{\mathrm{QM/MM}} = \sum_{i=1}^{n}\sum_{j=1}^{Q}\frac{-q_j}{r_{ij}} + \sum_{i=1}^{N}\sum_{j=1}^{Q}\frac{Z_i q_j}{r_{ij}} + E_{\mathrm{vdW}} + E_{\mathrm{bonded}} \tag{2}$$

The first term ensures that the QM wavefunction is polarized by all the surrounding point charges while the three remaining terms are the electrostatic interactions of the nuclei point charges, the QM/MM van der Waals interactions and some classical bonded terms involving bonds, angles and torsions (we chose to take into account all classical interactions involving at least one MM atom). As a basis for our QM/MM parameterization, we chose the Amber94 forcefield [16]. While in Amber electrostatic and van der Waals interactions are computed when two atoms are separated by at least three bonds, our QM subsystem feels all the MM point charges.

2.2 QM/MM frontier parameters

Because our primary target is to use a multireference ab initio level (like CASSCF or CASPT2) for the calculation of the QM part, it is out of reach to include the whole LRG group in the QM subsystem. Obviously, the minimal QM part is the whole π system of the chromophore, while lysine and glutamate are treated at the MM level. We chose to cut the lysine side chain between Cδ and Cε, thus including in the QM subsystem the whole retinal chromophore and the last bond of the lysine residue (Fig.1). As demonstrated in previous work [17] a motivation to cut this bond is that such a carbon–carbon bond is more appropriate when using a simple QM/MM frontier scheme like the link atom (LA) one. The LA scheme deals with the technical problem that arises when the frontier carbon–carbon covalent bond is cut: an electron remains unpaired on the QM side, which is not realistic. Consequently, the Cε atom is saturated with an hydrogen atom whose position is restrained on the Cδ–Cε line 1Å from the QM carbon atom. Numerous QM/MM studies have shown that in this case, the simple LA scheme (now LAH, where H indicates hydrogen) is accurate enough to design a smooth QM/MM frontier. Accordingly [17], we chose to let the LAH interact with all MM point charges, while no van der Waals or bonded terms were included between the LAH and the MM atoms.

The remaining part of the LRG group and the rest of the rhodopsin protein is treated with the Amber force field. While the Glu113 residue is entirely MM, Lys296 is now a mixed QM/MM residue, for which a special set of parameters should be derived. Moreover, Amber94 does

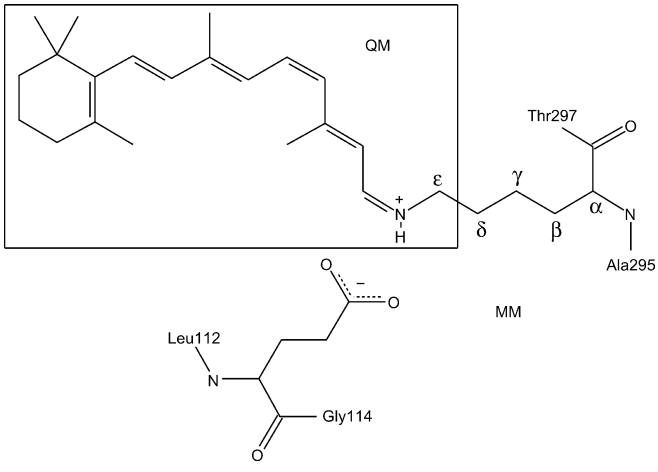

Fig. 1. Quantum mechanics(QM)/Molecular mechanics (MM) partition of the Lys296–ret–Glu113 molecular system in the rhodopsin protein

not contain any parameter for the centers of a conjugated chain. We derive such parameters for retinal.

All the QM/MM calculations were performed using a modified version of Gaussian98 [18], linked with a modified version of Tinker3.9 [19].

3 Parameterization

3.1. Selection of the QM/MM parameters

As already defined, the Lys296 residue is a mixed QM/MM molecular group and its MM parameters should be adapted to reflect this hybrid situation. We start with the reparameterization of the point charges. 1. While the original (protonated) Amber lysine residue has a net charge of +1, the MM side of the Lys296 residue must now have zero total charge because the positive charge belongs to the QM part. 2. As we used the LAH scheme, we have chosen to set to zero the Cδ point charge in order (1) not to overpolarize the QM/MM frontier and (2) to keep unchanged the classical parameters of the frontier (see later). 3. In order to keep a minimum of consistency with the Amber forcefield, the modified point charges were chosen to be as close as possible to the original ones.

With all these requirements in mind, we define empirically the set of modified point charges listed in Table 1. While all charges corresponding to the side chain remain unchanged (apart from Cδ set to 0), we decided to change the point charges carried by the carbonyl and the amino groups by about $\pm$0.05 electrons. Because the original restrained electrostatic potential (RESP) point charges for the amino and carbonyl groups of a peptide bond are large, we hope this modification will not affect too much the electrostatic interactions.

The QM/MM van der Waals interactions (defined in Amber by the parameters ε and R*) are really important to keep a realistic placement of the QM subsystem with respect to the protein cavity in which it lies. We therefore developed a set of atomic parameters for all the retinal chromophore atoms. Following the philosophy of the Amber forcefield, we will distinguish only three kinds of atoms in the chromophore: the carbon atoms of the π system, the other carbon atoms and the hydrogen atoms. Moreover, to limit the parameterization work, we kept the same ε values found in the original Amber forcefield for sp^2 carbon (0.0860), sp^3 carbon (0.1094) and hydrogen (0.0157).

The bond potential of the frontier includes the stretching term of the QM/MM frontier bond, and the angle terms N–Cε–Cδ, Hε–Cε–Cδ, Cε–Cδ–Hδ and Cε–Cδ–Cγ. The torsion terms involve rotations around three bonds (N–Cε, Cε–Cδ and Cδ–Cγ) as sketched in Fig. 2. All these potentials are already parameterized in Amber, with the exception of the dihedral angle C(ret)–N–Cε–Cδ which involves a retinal atom. In order to limit the reparameterization process, we decided to keep the same set of parameters in the QM/MM simulation. As mentioned previously, the charge of the Cδ atom was set to zero, thus it does not allow us to change the parameters of the frontier bond stretching potential: only this potential acts between the two atoms that make the bond. The QM/MM bond angles involve MM atoms with zero or very little charge; we can therefore hope that the original angle parameters are still valid for the hybrid region.

The torsion potentials are the most critical because they must be accurate enough to allow the molecular geometry to correctly relax during the photoisomerization. However, with the exception of C(Ret)-N-Cε-Cδ, all the QM/MM torsions are already parameterized in Amber and involve MM atoms with little charge. Thus we decided to determine the C(ret)–N–Cε–Cδ torsion parameters and the retinal van der Waals parameters together, in order to correctly reproduce the torsional behavior around the N–Cε (ϕ angle) and the Cε–Cδ (ψ angle) bonds for both the ground state (S_0) and the first singlet excited state (S_1) of the LRG system.

Table 1. Restrained ElectroStatic Potential (RESP) and Quantum Mechanics (QM)/Molecular Mechanics (MM) Lys296 point charges. MM modified values are given in *bold*

Atom	RESP	QM/MM
N	−0.3479	**−0.39805**
Cα	−0.2400	−0.2400
C	0.7341	**0.68395**
H	0.2747	**0.22455**
O	−0.5894	−0.63955
Hα	0.1426	0.1426
Cβ	−0.0094	−0.0094
Hβ	0.0362	0.0362
Cγ	0.0187	0.0187
Hγ	0.0103	0.0103
Cδ	−0.0479	**0.0000**
Hδ	0.0621	0.0621
Cε	−0.0143	
Hε	0.1135	
Nζ	−0.3854	
Hζ	0.3400	
Total charge	*+1*	0

3.2 Fitting procedure and resulting parameters

In order to determine the missing parameters defined earlier, one needs to determine the correct S_0 and S_1 energy surfaces by computing them at the QM level only. In particular one has to scan the (ϕ,ψ) space, i.e.

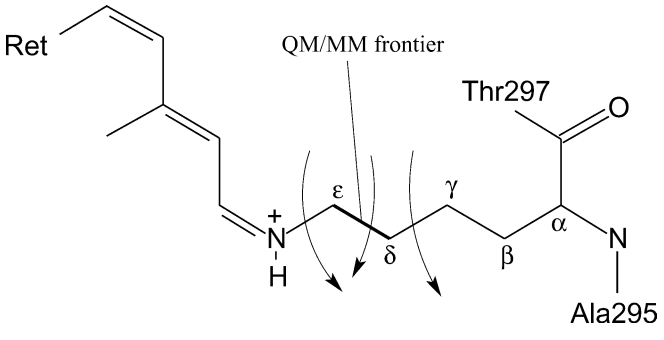

Fig. 2. QM/MM torsions it (*curved arrows*)

calculate the S_0 and S_1 energies for each pair of (ϕ,ψ) values. Since performing such calculations for the entire retinal and lysine molecular system would be computationally expensive, we built a model system in which the retinal chromophore is replaced by a three conjugated double bonds Schiff base, linked to a lysine-like residue that contains only three bonds in the side-chain (instead of five). The model and the (ϕ,ψ) angles are displayed in Fig. 3. The initial structure is defined via geometry optimization of the model at the RHF/6-31G* level, leading to $\phi = -120.726°$and $\psi = 179.704°$. Then a grid of 96 different structures is built, varying ϕ from $-120.726°$ to 44.274° with a step of 15° and ψ from 179.704° to 74.704° with a step of $-15°$. For each structure, four energy calculations are performed: CAS(6,6)/6-31G* on the ground state and on the first singlet excited state and QM/MM CAS(6,6)/6-31G*/Amber computation on the same states. The root mean square of the difference between the QM and QM/MM relative energies (where relative means with respect to their minimum) is then minimized (using the simplex method) by running MM calculations for the van der Waals interactions between the QM and MM parts and the C(ret)–N–Cε–Cδ torsion. The resulting optimized van der Waals atomic parameters (R* in angströms; ε in kilocalories per mol) are: (1.8700; 0.0860) for a carbon atom in the conjugated π system (1.8700; 0.1094) for the other carbon atoms and (0.9200; 0.0157) for a hydrogen atom. The C(ret)–N–Cε–Cδ torsional potential is given by:

$$0.750[1 + cos\phi] \quad (3)$$

The original QM and the resulting parameterized QM/MM potential energy surfaces for both S_0 and S_1 states are reported in Fig. 4. Differences between QM and QM/MM energies exceed 3 kcal/mol for only 11 structures in S_0 and for nine structures in S_1 over a total number of 96 structures. However these structures have very high relative energies and should never be reached during a geometry optimization.

In conclusion we designed a QM/MM Lys296–ret potential that reproduces efficiently the torsional behavior of the lysine side-chain at the QM/MM frontier. The next step in the building of our QM/MM LRG system regards the quality of the retinal–Glu113 interactions, when the glutamate counterion is replaced with Amber point charges.

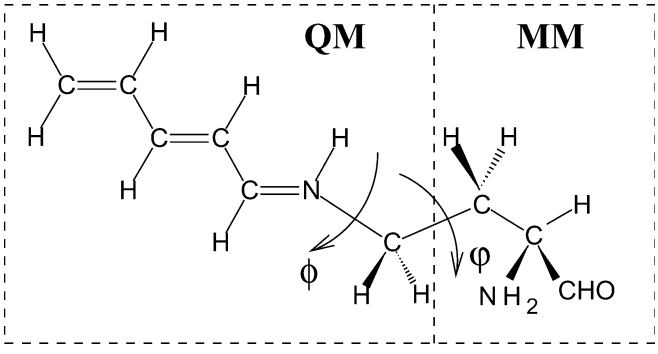

Fig. 3. Model system for the fitting procedure of the Lys296–retinal parameters

4 Suitability of the RESP point charges

As already reported, our QM/MM LRG system includes the whole counterion in the MM subsystem, which is treated according to the Amber forcefield. In this

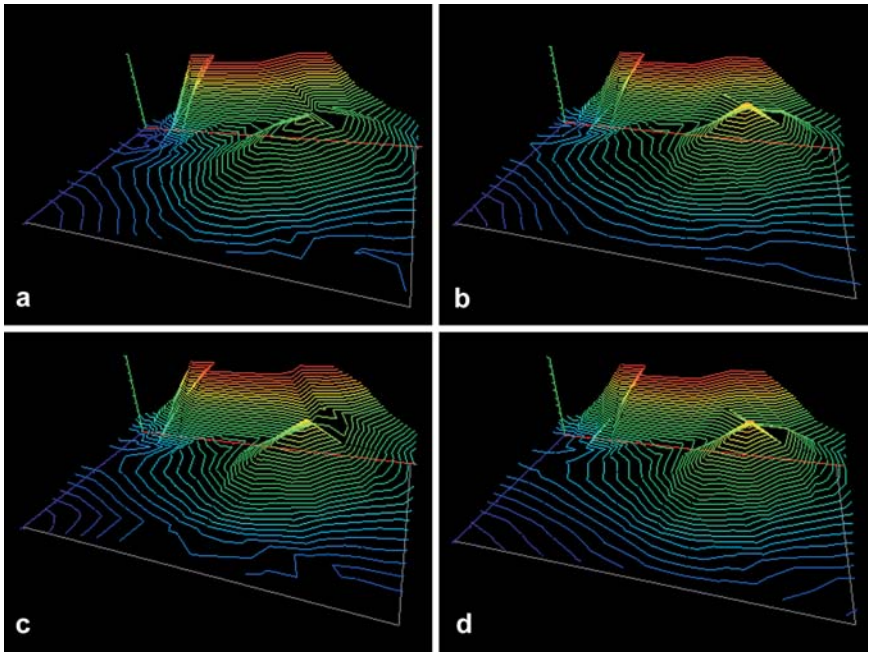

Fig. 4. Potential energy surfaces (the *red axis* corresponds to the ϕ angle, the *blue axis* corresponds to the ψ angle, the *green axis* corresponds to the energy relative to its minimum at $\phi = -120.726°; \psi = 179.704°$)

forcefield, the non-bonded electrostatic interactions are modeled by an atom-centered point charges, determined according to the (RESP) procedure [20]. This procedure comes from the original ESP scheme of Cox and Williams, in which a least square fitting algorithm is used to compute a set of charges that reproduce the electrostatic potential calculated on a grid of points surrounding the molecule of interest. Basically, the RESP improvement consists in a penalty function that restrains the charges on non-hydrogen atoms, in order to lower the conformational dependance of the fitted charges (typically this is the case for alkyl carbon atoms).

The RESP charges have often proven their reliability (e.g., recently in [21]) both in MM and QM/MM computations (using both semiempirical and ab initio Hamiltonians). However, in the present QM/MM work, the corresponding Glu113 point charges must be able to correctly reproduce the interactions between the retinal chromophore and its counterion (both in the ground state and in the excited state). Therefore we decided to compare QM and QM/MM geometries and energies of a retinal model interacting with a counterion model. The corresponding model system is displayed in Fig. 5: the retinal chromophore is modelled by the 4-*cis*-nonatetraeniminum cation always computed at the CASSCF and CASPT2 (10 electrons in 10 orbitals, using the 6-31G* basis set) levels of theory while the counterion model is an acetate anion. The relative orientation and distance between the chromophore and its counterion for this molecular complex are derived from the crystallographic structure of rhodopsin where the retinal chromophore is replaced by our model with a geometry optimized in vacuo and the Glu113 side chain is cut between the Cα and Cβ atoms and saturated with a hydrogen atom (i.e., an acetate anion).

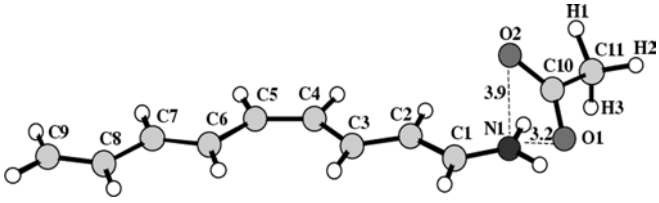

Fig. 5. Model chromophore and counterion used for restrained electrostatic potential charge validation

Table 2. Acetate RESP charges. The atom numbers are given in Fig. 5. For comparison purposes, Amber RESP charges for glumate are also given

Atom	Acetate RESP	Glu RESP
O1	−0.8661	−0.8188
O2	−0.8538	−0.8188
C10	0.9239	0.8054
C11	−0.2943	
H1	0.0301	
H2	0.0301	
H3	0.0301	

To derive RESP charges for the acetate ion, we used the fitting program freely downloadable from the Amber site [22]. From the starting geometry defined previously, we took the acetate alone and carried out an energy calculation at the RHF/6–31G* level of theory to obtain four shells of points on which the electrostatic potential due to the acetate is calculated. The derived RESP charges are reported in Table 2. Notice that the charges carried by the carbon and oxygen atoms are similar to the ones defined in the Amber forcefield for the glutamate anion.

At this point, QM and QM/MM calculations can be compared. Two kinds of computational tests (denoted as Exp1 and Exp2 in the following) were carried out:

Exp1: Optimization of the ground state (S_0) geometry of the model chromophore (acetate frozen) and energy gap calculations.

Exp2: Optimization of the first excited state (S_1) geometry of the model chromophore (acetate frozen) and energy gap calculations.

In both Exp1 and Exp2, the orientation and the distance of the model chromophore with respect to the acetate are constrained to the initial values. While geometry optimizations are performed at the CASSCF level (including the whole π system), dynamical correlation is included carrying out CASPT2 calculations using the Molcas-5 program [23]. First, it should be noted that the QM and QM/MM geometries are in very close agreement (see bond lengths for the chromophore in Table 3). The starting geometry is planar and remains planar both in S_0 and in S_1. In Table 4 we report the energy gaps between the ground state and singlet excited states computed at the CASSCF and CASPT2 levels, using a three or four roots state-averaged CASSCF wavefunctions (S_0, S_1, S_2 and also S_3 for Exp2) in order to ensure the presence of the absorbing state, identified through a large oscillator strength value between S_0 and this state. Actually, S_0 and S_1 are states of the same kind (i.e. S_1 is not the absorbing ionic state found both in vacuo [7] and in the protein environment [15]). Thus the main effect of the counterion is to stabilize the non absorbing states with respect to the spectroscopic one. Inspection of the CASSCF gaps for the two computational experiments clearly shows that a pure-electrostatic model of the

Table 3. Model chromophore optimized bond lengths (Å)

Experiment	N1–C1	C1–C2	C2–C3	C3–C4	C4–C5	C5–C6	C6–C7	C7–C8	C8–C9
Exp1 QM	1.282	1.443	1.355	1.452	1.358	1.456	1.353	1.459	1.346
Exp1 QM/MM	1.283	1.441	1.356	1.451	1.358	1.455	1.353	1.459	1.346
Exp2 QM	1.303	1.408	1.441	1.382	1.436	1.395	1.443	1.380	1.427
Exp2 QM/MM	1.303	1.407	1.440	1.381	1.437	1.394	1.443	1.380	1.427

Table 4. Complete-active-space self-consistent-field (CASSCF) and second order multireference many body perturbation theory using a CASSCF reference (CASPT2) (10,10)/6-31G* energy gaps (kcal.mol^{-1}). The numbers in bold highlight the absorbing state (oscillator strength f > 0.7 ; the non absorbing states all have f < 0.2)

	Exp1		Exp2	
	QM	QM/MM	QM	QM/MM
CASSCF($S_0 \rightarrow S_1$)	101.0	100.0	61.2	61.5
CASSCF($S_0 \rightarrow S_2$)	**116.2**	**113.2**	95.3	**94.0**
CASSCF($S_0 \rightarrow S_3$)			**98.0**	95.8
CASPT2($S_0 \rightarrow S_1$)	82.7	79.9	57.5	57.8
CASPT2($S_0 \rightarrow S_2$)	**84.3**	**85.2**	**62.6**	**64.0**
CASPT2($S_0 \rightarrow S_3$)			89.0	86.3

Table 5. CASSCF Mulliken charges for the model chromophore reported as a percentage of the total positive charge located on the half of the model chromophore located near the counterion. States are ordered following the CASPT2 energy levels. The numbers in bold highlight the absorbing state

	Exp1		Exp2	
	QM	QM/MM	QM	QM/MM
S_0	92	91	87	87
S_1	62	64	86	86
S_2	**53**	**58**	**35**	**44**
S_3			87	82

counterion reproduces quite well the corresponding QM values: the QM/MM results always differ by less than 4 kcal.mol^{-1}. However, two distinctive features can be highlighted:

- QM and QM/MM energy gaps between S_0 and the non absorbing excited states (i.e. states with little oscillator strength) are in very good agreement (differences less than 1 kcal.mol^{-1}).
- QM and QM/MM energy gaps between S_0 and the spectroscopic state (i.e. the state with a large oscillator strength value) differ more (the QM/MM excited state is always slightly stabilized with respect to the QM one, in a range from 2 to 4 kcal.mol^{-1}).

Notice that, owing to near degeneracy of the third and fourth roots in Exp2, the QM absorbing state is S_3 while it is S_2 in the corresponding QM/MM. Looking at the CASPT2 values, the tendencies are the same for the covalent states and show a little stabilization of these states when the QM/MM scheme is used. However, the QM/MM ionic states are now slightly destabilized with respect to the QM ones. Remarkably, owing to some cancellation errors that we will discuss in the following, the QM/MM CASPT2 energy gaps are now closer to the QM ones (differences always less than 1.5 kcal.mol^{-1}). To summarize, our QM/MM scheme seems to overstabilize the absorbing state at the CASSCF level. However, CASPT2 energy gaps recover this overstabilization yielding a slightly understabilized value. The proposed CASPT2//CASSCF/Amber strategy is thus validated.

The positive cancellation effect discussed earlier can be rationalized by looking at the Mulliken charges. First it should be noted that in all the QM calculations, some charge transfer takes place between the chromophore and the acetate (the chromophore always has a total charge about 0.9) which, obviously, cannot be treated using a point charge model of the counterion. For this reason, in Table 5 we have reported the percentage of Mulliken charges located on the half of the chromophore closest to the counterion (i.e. N_1 to C_4 ; see figure 5 for notation) with respect to the total charge. While these relative Mulliken charges are in very close agreement for the corresponding QM and QM/MM non absorbing states, the discrepancy is larger in the case of the spectroscopic state. In fact, in the QM/MM model, there is less charge flow towards the hydrocarbon end of the chromophore. Thus, at the CASSCF level, the QM/MM absorbing state is stabilized, with respect to the QM one, by the interaction with the counterion, while the final destabilization of this state at the CASPT2 level is more difficult to rationalize. We provide here a tentative explanation. Since, in general, the dynamic correlation effect tends to stabilize the excited states with ionic character, with respect to those with covalent character, the counterion overstabilization is somehow recovered, probably owing to an increase of the charge flow towards the hydrocarbon end in the hypothetical corresponding CASPT2 wavefunction.

5. Conclusions

In the present work, we defined, parameterized and validated a QM/MM forcefield ultimately devoted to the study of the excited state motion of the retinal chromophore in the rhodopsin cavity. We focused on the molecular system composed of the chromophore, the lysine residue linked to retinal through a protonated Schiff base and its counterion (a glutamate anion). The main characteristics of the resulting QM/MM model are

- The QM subsystem is restricted to the retinal chromophore and the last bond of the lysine sidechain, and thus includes the protonated Schiff base linkage. The validated level of theory is a CASPT2//CASSCF level that includes the whole π system in the active space.
- The MM subsystem contains the rest of the protein, including the protonated Schiff base counterion and it is treated using the Amber forcefield.
- The QM/MM frontier has been carefully parameterized: modified RESP charges for the lysine MM atoms and torsional and van der Waals parameters are derived to get a correct description of the torsional potential of the frontier bonds both in S_0 and S_1.
- The use of the Amber-like charges of an acetate anion (mediating the electrostatic interaction with retinal) has been tested and validated.

The QM/MM model defined here has recently been applied to a model of the rhodopsin protein at the CASPT2//CASSCF/Amber level of theory [15] and

allowed the spectroscopic features of rhodopsin to be qualitatively reproduced and explained.

Acknowledgements. Funds were provided by the Università di Siena (Progetto di Ateneo 02/04) and HFSP (RG 0229/2000- M). N.F. is grateful for the EU Grant HPMF-CT-2001-01769. We thank CINECA for granted calculation time.

References

1. Mathies RA, Lugtenburg J (2000) In: Stavenga DE, DeGrip WJ, Pugh En Jr (eds) Handbook of biological physics Vel 3 Elsevier p. 55–90.
2. Kandori H, Shichida Y, Amstedam Yoshisawa T (2001) Biochemistry (Moscow) 66:1197
3. Garavelli M, Celani P, Bernardi F, Robb MA, Olivucci M (1997) J Am Chem Soc 119:6891
4. Garavelli M, Vreven T, Celani P, Bernardi F, Robb MA, Olivucci M (1998) J Am Chem Soc 120:1285
5. Garavelli M, Negri F, Olivucci M (1999) J Am Chem Soc 121:1023
6. Garavelli M, Bernardi F, Robb MA, Olivucci M (1999) J Mol Struct (THEOCHEM) 463:59
7. Gonzàlez-Luque R, Garavelli M, Bernardi F, Merchán M, Robb MA, Olivucci M (2000) Proc Natl Acad Sci USA 97:9379
8. Han M, Smith SO (1995) Biophys Chem 56:23
9. Bifone A, de Groot HJ M, Buda F (1997) J Phys Chem B 101:2954
10. Yamada A, Kakitani T, Yamamoto S, Yamato T (2002) Chem Phys Lett 366:670
11. Röhrig UF, Guidoni L, Rothlisberger U (2002) Biochemistry 41:10799
12. Sugihara M, Buss V, Entel P, Elstner M, Frauenheim T (2002) Biochemistry 41:15259
13. Okada T, Ernst OP, Palczewski K, Hofmann KP (2001) Trends Biochem Sci 26:318
14. Teller DC, Okada T, Behnke CA, Palczewski K, Stenkamp RE (2001) Biochemistry 40:7761
15. Ferré N, Olivucci M (2003) J Am Chem Soc 125:6868
16. Cornell WD, Cieplak P, Bayly CI, Gould IR, Merz KM, Jr Ferguson DM, Spellmeyer DC, Fox T, Cladwell JW, Kollman PA (1995) J Am Chem Soc 117:5179
17. Ferré N, Olivucci M (2003) J Molec Struct (Theochem) 632:71
18. Frisch MJ, Trucks GW, Schlegel HB, Scuseria GE, Robb MA, Cheeseman JR, Zakrzewski VG, Montgomery JA, Jr Stratmann RE, Burant JC, Dapprich S, Millam JM, Daniels AD, Kudin KN, Strain MC, Farkas O, Tomasi J, Barone V, Cossi M, Cammi R, Mennucci B, Pomelli C, Adamo C, Clifford S, Ochterski J, Petersson GA, Ayala PY, Cui Q, Morokuma K, Malick D, Rabuck A, Raghavachari K, Foresman J, Cioslowski J, Ortiz J, Baboul A, Stefanov B, Liu G, Liashenko A, Piskorz P, Komaromi I, Gomperts R, Martin R, Fox D, Keith T, Al-Laham M, Peng C, Nanayakkara A, Gonzales C, Challacombe M, Gill P, Johnson B, Chen W, Wong M, Andres J, Gonzales C, Head-Gordon M, Replogle E, Pople J (1998) Gaussian 98, revision A.9 Gaussian, Pittsburgh, PA
19. Ponder JW (2001) Tinker 3.9 – software tools for molecular design. http://dasher.wustl.edu/tinker/
20. Bayly CI, Cieplak P, Cornell WD, Kollman PA (1993) J Phys Chem 97:10269
21. Laio A, Vande Vondele J, Rothlisberger U (2002) J Phys Chem B 106:7300
22. http://www.amber.ucsf.edu/amber/questions/resp.html
23. Andersson K, Barysz M, Bernhardsson A, Blomberg M RA, Cooper DL, Fülscher MP, deGraaf C, Hess BA, Karlström G, Lindh R, Malmqvist PA, Nakajima T, Neogrády P, Olsen J, Roos BO, Schimmelpfennig B, Schütz M, Seijo L, Serrano-Andrés L, Siegbahn P EM, Stålring J, Thorsteinsson T, Veryazov V, Widmark PO (2002) Molcas version 5.4 Lund University, Sweden